

# Energy sharing and asymmetry parameters for photo double ionization of Helium 100 eV above threshold in single particle and Jacobi coordinates

A. Knapp<sup>1</sup>, M. Walter<sup>2</sup>, Th. Weber<sup>1</sup>, A. L. Landers<sup>3</sup>, S. Schössler<sup>1</sup>, T. Jahnke<sup>1</sup>, M. Schöffler<sup>1</sup>, J. Nickles<sup>1</sup>, S. Kammer<sup>1</sup>, O. Jagutzki<sup>1</sup>, L. Ph. H. Schmidt<sup>1</sup>, T. Osipov<sup>4</sup>, J. Rösch<sup>5,1</sup>, M. H. Prior<sup>5</sup>, H. Schmidt-Böcking<sup>1</sup>, C. L. Cocke<sup>4</sup>, J. Feagin<sup>6</sup> and R. Dörner<sup>1\*</sup>

<sup>1</sup> *Institut für Kernphysik, University Frankfurt,  
August-Euler-Str. 6, D-60486 Frankfurt, Germany*

<sup>2</sup> *Fakultät für Physik, University Freiburg, Hermann-Herder-Str. 3, Germany*

<sup>3</sup> *Dept. of Physics, Western Michigan Univ., Kalamazoo, MI 49008*

<sup>4</sup> *Dept. of Physics, Kansas State Univ,  
Cardwell Hall, Manhattan KS 66506*

<sup>5</sup> *Lawrence Berkeley National Lab., Berkeley CA 94720*

<sup>6</sup> *Department of Physics, California State University-Fullerton, Fullerton, California 92834*

(Dated: October 22, 2002)

## Abstract

We present a joint experimental and theoretical study of the double differential cross section for the double ionization of helium by absorption of one 179 eV linear polarized photon (100 eV above threshold). We show the energy sharing and the asymmetry parameters in both single particle coordinates and in Jacobi coordinates. An asymmetric sharing of the electron excess energy and a breakup of the electron pair preferentially parallel to the polarization axis is found. This marks a deviation from the propensity rule favoring perpendicular relative electron motion which has been observed to hold at energies closer to the double ionization threshold.

---

\*Electronic address: doerner@hsb.uni-frankfurt.de

Double ionization of helium by single photon absorption is a benchmark process for the investigation of electron-electron correlation in few-body systems. The three particles final state is completely kinematically determined by a set of 5 linear independent degrees of freedom (the remaining 4 are fixed by momentum and energy conservation). This fivefold differential cross section can be reduced by one degree of freedom by taking the dipole approximation into account. For examination within the dipole approximation it is helpful to integrate over 2 or 3 of the degrees of freedom to obtain doubly or singly differential cross sections. These cross sections give an overview of which regions of this 4 dimensional phase space are most important. The cross section differential in an arbitrary momentum vector  $\vec{k}$  can be described by only two parameters, the cross section differential in energy  $d\sigma/dE$  and the asymmetry parameter  $\beta$ . It can always be expressed in the simple form

$$\frac{d\sigma}{dE d\hat{k}} = \frac{1}{4\pi} \frac{d\sigma}{dE} \left(1 + \beta P_2(\hat{\epsilon} \cdot \hat{k})\right) \quad (1)$$

. Here  $\hat{\epsilon}$  is the linear light polarization axis and  $P_2$  the second legendre polynomial. While such cross sections are extremely valuable for the characterization of the process, there has been only three experiments reported [1-3].

Two coordinate sets are widely used in the literature to describe the momentum configurations: The first set is the electron momenta  $\vec{k}_{1,2}$  relative to the center of mass of all particles with the excess energy given by  $E_{excess} = E_1 + E_2$  and  $E_{1,2} = k_{1,2}^2/2$ . The second set is the Jacobi momenta - the center of mass momentum of the electron pair  $\vec{k}_+ = \vec{k}_1 + \vec{k}_2$ , where  $-\vec{k}_+$  is the momentum of the recoiling nucleus, and  $\vec{k}_- = (\vec{k}_1 - \vec{k}_2)/2$  is the relative momentum of the electrons. The excess energy shared in the corresponding energies reads  $E_{excess} = E_+ + E_-$  with  $E_+ = k_+^2/4$  and  $E_- = k_-^2$ . Atomic units are used throughout.

The two coordinate systems suggest two different perspectives on the double ionization process: single electron coordinates describe the escape of each electron from the nuclear potential. Therefore they would be most appropriate if the coupling between the electrons could be treated as perturbation while their motion is mainly governed by the nuclear field and the photon. This can be expected for example at very high photon energies, where one expects [4, 5] that one electron absorbs the majority of the photon energy and angular momentum while the second electron is emitted with little energy either via a shake-off or is knocked out in a binary collision by the fast electron. In contrast, Jacobi coordinates are better suited to describe the motion of the nucleus ( $k_+$ ) in the potential of the electron pair

and the breakup of the two electrons ( $k_-$ ). This is most useful if the saddle region of the potential surface governs the final state of the reaction, which is expected close to threshold [6]. It has been shown experimentally that just above threshold the ionic motion tends to freeze out on the saddle [2] ( $E_+ \ll E_-$ ). In addition, the ionic motion maximizes along the polarization axis ( $\beta_+ > 0$ ) while the electron pair breaks up predominantly perpendicular to the polarization ( $\beta_- < 0$ ). This can be understood by a Wannier type analysis, which predicts, that double ionization near threshold can only be reached if ionic and electron motion are perpendicular, all other cases lead to single ionization [6–12].

The preferential break up of the electron pair can also be understood by studying the helium atom in a molecular picture, where the electronic separation  $\vec{R}$  is interpreted as a molecular axis and the projection  $m$  of the total angular momentum on this axis is taken as an approximate quantum number. This analysis was performed in [13] where some misprints appeared, so we repeat it briefly here. Apart from  $m$ , the other quantum number to classify molecular symmetries is  $t = 0, 1$ . If we denote the position of the electronic center of mass relative to the nucleus by  $\vec{r}$ ,  $(-1)^t$  describes the electronic wave functions behaviour under the internal parity transformation  $\vec{r} \rightarrow -\vec{r}$ . In this picture the helium ground state is a molecular  $\sigma_g$  state ( $m = 0$  and  $t = 0$ ) and dipole selection rules allow transition to  $\sigma_u$  ( $m = 0$  and  $t = 1$ ) or  $\pi_u$  ( $m = 1$  and  $t = 1$ ) molecular states. A propensity rule, first found in double excitation and also valid for double ionization near threshold, can be expressed as

$$\Delta((-1)^{t+m}) = 0. \quad (2)$$

Hence  $\pi_u$  and therefore final states with  $m = 1$  are preferred. This propensity rule is also valid in momentum space, where  $\vec{k}_-$  takes the role of the molecular axis. The corresponding asymmetry parameter is  $\beta_- = 2$  for pure  $m = 0$  and  $\beta_- = -1$  for pure  $m = 1$  transitions. Data for 1 eV [2] and 20 eV [3] above threshold agree with the dominance of  $m = 1$  but the propensity rule is expected to break down at higher energies [13].

In the present study we have measured doubly differential cross sections at  $E_{excess} = 100$  eV above threshold. The experiment has been performed using Cold Target Recoil Ion Momentum Spectroscopy (COLTRIMS) (see [14] for a recent review) at beamline 4.0 at the Advanced Light Source (ALS) at the Lawrence Berkeley National Laboratory [15] during double bunch mode operation. In brief, the linear polarized photon beam (Stokes parameter  $S_1 > 0.99$ ) is intersected with a supersonic Helium gas jet. The  $\text{He}^{2+}$  ions and electrons

created in the overlap volume of about  $0.5 \text{ mm}^3$  are guided by electric and homogeneous magnetic fields onto large area position sensitive channel plate detectors with delay-line anode [16]. The momentum vector of each particle of a coincident pair ( $\text{He}^{2+}$  and one electron) is then calculated from the measured time-of-flight and the position of impact of each on their separate detectors. In order to focus in three dimensions an acceleration region (7.61 V/cm) with a lens followed by a drift region is used for the recoiling ions (see e.g. [14]). The electric and magnetic field (13.3 G) yield a solid angle of  $4\pi$  for collection of electrons up to 60 eV. The momentum of the other electron is deduced from total momentum conservation of the three particle final state. With an excess energy of 100 eV, always one electron has less than 50 eV, and hence our setup covers the full 5 dimensional final state momentum space of the reaction. This allows the choice of any set of coordinates for display of the results and also integration over any number of coordinates desired.

The calculations shown use a 3C wave function [17] to describe the correlated three particle final state. The matrix elements are calculated using the dipole operator in velocity and length form to test for possible gauge dependencies. The method of integration to obtain energy distributions and  $\beta_{\pm}$  parameters is described in [13].

Figure 1 shows the momentum space distribution in  $k_1$ ,  $k_+$  and  $k_-$  for three different photon energies. The right column displays the present results for the momentum distributions in  $k_1$ ,  $k_+$  and  $k_-$  for an energy of 100 eV above threshold. These results should be compared to previous measurements with lower photon energy: the left and the middle columns of Figure 1 show the results for 1 eV and 20 eV above threshold, from [2] and [3]. The z and y components of the momentum are plotted on the horizontal and vertical axes, respectively. The polarization axis in all images is horizontal and the photon propagation is perpendicular to y and z. The plots are projections onto the y-z plane with  $-0.1 < k_x < 0.1$  a.u. for the 1 eV data set and  $-0.2 < k_x < 0.2$  a.u. for the 20 eV data. In the right column (100 eV above threshold) only events with a momentum component perpendicular to the plane of less than 1 a.u. are plotted. Such a cut through a sphere instead of a full projection of the sphere onto a plane prevents the typical structure from being buried by events which are located out of the selected plane. Already in these data one can see that at 100 eV above threshold the slow electrons are almost isotropic, whereas the fast electrons are preferentially emitted along the polarization axis. The momentum of the recoiling ion has a strong dipole character. The  $k_-$  distribution also shows a maximum along the polarization

axis, i.e. the electron pair break up preferentially along the polarization axis  $\epsilon$ . The latter is in contrast to the situation at 1 eV and 20 eV above threshold, where one finds, that the  $k_-$  distribution has maxima perpendicular to the polarization axis, i.e. the electron pair break up preferentially perpendicular to  $\epsilon$ . This observation shows that the propensity rule for the molecular states with  $|m| = 1$  no longer holds 100 eV above threshold.

To investigate the situation in more detail figure 2 and 3 show the doubly differential cross sections in electron and Jacobi coordinates. For the electron energy distribution we find a pronounced U-shape, i.e. a very asymmetric energy sharing. At the same time the momentum of the fast electron exhibits almost a dipole angular distribution while the slow electron has a  $\beta$  close to 0 or even negative. This indicates that at least for very asymmetric energy sharing to a fair approximation one can state that the fast electron has absorbed the photon energy and most of the angular momentum. In Jacobi coordinates (figure 3) one finds that the energy is about equally shared between the center of mass motion ( $E_+$ ) and the electron pair breakup motion ( $E_-$ ), in contrast to the situation close to threshold where  $E_+ \ll E_-$  is favored due to electron repulsion [2]. At the same time  $\beta_+$  is almost 2 in good agreement between theory and experiment.  $\beta_+$  however varies only little with the excess energy, showing just a slight structure in the region of  $E_+ \approx E_{excess}/2$  [18]. This structure can be explained by the contribution of configurations where either  $k_1$  or  $k_2 \rightarrow 0$  and therefore the corresponding Coulomb density-of-states factor diverges [13].

The physical interpretation for the nearly dipolar angular distribution of the recoil ion, almost independent of the photon energy, is, that the dipole operator (photon) has to couple to a charge dipole in the atom. No matter what the details of the electron-electron correlation are, the nucleus is always one end of the charge dipole which absorbs the photon and hence its momentum distribution reflects the angular characteristics of this first step of photon absorption.

The  $\beta_-$  parameter is not negative anymore in the region which contributes most to the total cross section. This indicates that the propensity rule for  $\pi_u$  final states no longer holds at 100 eV, as it does up to 20 eV excess energy [3]. A structure around  $E_+ \approx E_{excess}/2$  is shown in the calculations which is not seen in the experiment. The reason for this discrepancy is unclear but may show the difficulty of describing the three particle Coulomb continuum particularly at unequal energy sharing conditions [19, 20].

In summary we have measured doubly differential cross sections evaluated in single elec-

tron and Jacobi coordinates and compared to theoretical calculations. Theory and experiment are in good agreement especially in the observed breakdown of the propensity rule favoring  $m = 1$  at 100 eV. Without this propensity the main motivation for analyzing the process in Jacobi coordinates is lost. The evolution of the three-body system is no longer governed by the saddle region of the potential. In contrast, the asymmetry in the electron energy distribution and the large positive  $\beta_1$  of the faster electron are better demonstrated in single electron coordinates. The energy sharing and angular distribution favor the picture of one electron absorbing the photon energy and its angular momentum followed by a transfer of a small fraction of the energy to the second electron.

### Acknowledgments

This work was supported in part by BMBF, DFG, the Division of Chemical Sciences, Geosciences and Biosciences Division, Office of Basic Energy Sciences, Office of Science, U. S. Department of Energy. R.D. was supported by the Heisenberg Programm der DFG. A. K. and Th.W. thank Graduiertenförderung des Landes Hessen for financial support. We thank E. Arenholz and T. Young and the staff of the Advanced Light Source for extraordinary support during our beam time. M.W. was supported by TPA1 in the DFG Sonderforschungsbereich 276 of the University of Freiburg. M.W. wants to thank J.S. Briggs for reading the manuscript.

- 
- [1] R. Wehlitz, F. Heiser, O. Hemmers, B. Langer, A. Menzel and U. Becker. *Phys. Rev. Lett.* **67**, 3764 (1991).
  - [2] R. Dörner, J. Feagin, C.L. Cocke, H. Bräuning, O. Jagutzki, M. Jung, E.P. Kanter, H. Khemliche, S. Kravis, V. Mergel, M.H. Prior, H. Schmidt-Böcking, L. Spielberger, J. Ullrich, M. Unverzagt and T. Vogt. *Phys. Rev. Lett.* **77**, 1024 (1996). see also erratum in *Phys. Rev. Lett.* **78**, 2031 (1997).
  - [3] H.P. Bräuning, R. Dörner, C.L. Cocke, M.H. Prior, B. Krässig, A. Bräuning-Demian, K. Carnes, S. Dreuil, V. Mergel, P. Richard, J. Ullrich and H. Schmidt-Böcking. *J. Phys.* **B30**, L649 (1997).

- [4] A. Knapp, A. Kheifets, I. Bray, Th. Weber, A. L. Landers, S. Schössler, T. Jahnke, J. Nickles, S. Kammer, O. Jagutzki, L. Ph. Schmidt, T. Osipov, J. Rösch, M. H. Prior, H. Schmidt-Böcking, C. L. Cocke and R. Dörner. *Phys. Rev. Lett.* **89**, 033004 (2002).
- [5] Z.J. Teng and R. Shakeshaft. *Phys. Rev.* **A49**, 3597 (1994).
- [6] G.H. Wannier. *Phys. Rev.* **90**, 817 (1953).
- [7] J.M. Feagin. *J. Phys.* **B29**, L551 (1996).
- [8] A. Huetz, P. Selles, D. Waymel and J. Mazeau. *J. Phys.* **B24**, 1917 (1991).
- [9] J.M. Feagin. *J. Phys.* **B28**, 1495 (1995).
- [10] A.K. Kazanski and V.N. Ostrovsky. *Phys. Rev.* **A51**, 3712 (1995).
- [11] A.K. Kazanski and V.N. Ostrovsky. *Phys. Rev.* **A48**, R871 (1993).
- [12] A.K. Kazanski and V.N. Ostrovsky. *J. Phys.* **B27**, 447 (1994).
- [13] J.S. Briggs, M. Walter and J.M. Feagin. *J. Phys. B: At. Mol. Opt. Phys.* **33**, 2907 (2000).
- [14] R. Dörner, V. Mergel, O. Jagutzki, L. Spielberger, J. Ullrich, R. Moshhammer and H. Schmidt-Böcking. *Physics Reports* **330**, 96–192 (2000).
- [15] A.T. Young, J. Feng, E. Arenholz, H.A. Padmore, T. Henderson, S. Marks, E. Hoyer, R. Schlueter, J.B. Kortright, V. Martynov, C. Steier, and G. Portmann, *Nucl. Instr. Meth.* **A467-468**, 549 (2001).
- [16] (see Roentdek.com for details of the detectors).
- [17] M. Brauner, J. S. Briggs, and H. Klar. *J. Phys. B* **22**, 2265–2287 (1989).
- [18] M Pont and R. Shakeshaft *Phys. Rev. A* **54**, 1448–51 (1996).
- [19] F. Maulbetsch, M. Pont, J. S. Briggs, and R. Shakeshaft. *J. Phys. B* **28**, L341 (1995).
- [20] C. Dawson, S. Cvejanovic, D. P. Seccombe, T. J. Reddish, F. Maulbetsch, A. Huetz, J. Mazeau and A. S. Kheifets. *J. Phys. B* **34**, L525 (2001).

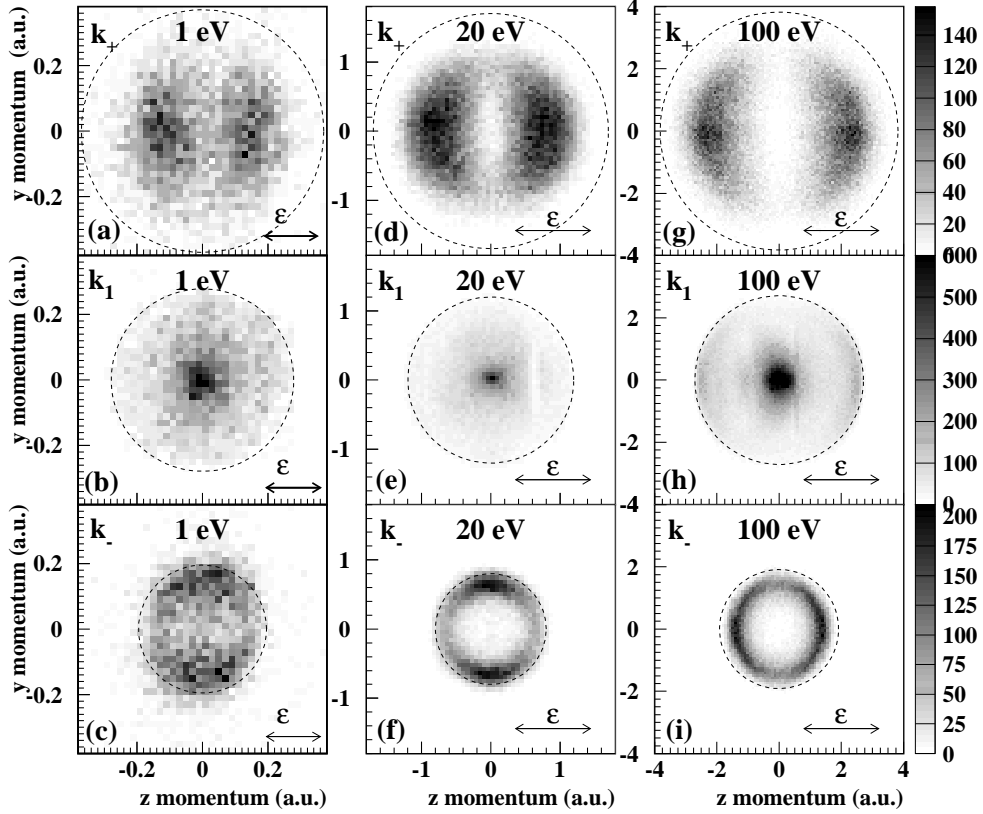


FIG. 1: Density plots of projections of the momentum distributions from double ionization of He by three different energies, from left to right: data sets for 1 eV, 20 eV and 100 eV above threshold. The data for 1 eV and 20 eV (left and middle column) are previous measurements, see also [2, 3]. The measurement at 100 eV above threshold is displayed in the right column. The  $z$  and  $y$  components of the momentum are plotted on the horizontal and vertical axes, respectively. The polarization vector of the photon is in the  $z$  direction and the photon propagates in the  $x$  direction perpendicular to  $y$  and  $z$ . The plots are projections onto the  $y$ - $z$  plane with  $-0.1 < k_x < 0.1$  a.u. for the 1 eV data set,  $-0.2 < k_x < 0.2$  a.u. for the 20 eV data and for the 100 eV above threshold measurement only events with  $-1 < k_x < 1$  a.u. are projected onto the plane. (a),(d),(g) Momentum distribution of the  $He^{2+}$  ion ( $k_+$ ) for 1 eV, 20 eV and 100 eV above threshold. (b),(e),(h) electron momentum ( $k_1$ ) and (c),(f),(i) electron pair relative momentum  $(k_1 - k_2)/2$ . The circle locates the maximum possible momentum in each coordinate at the respective Photon energy.

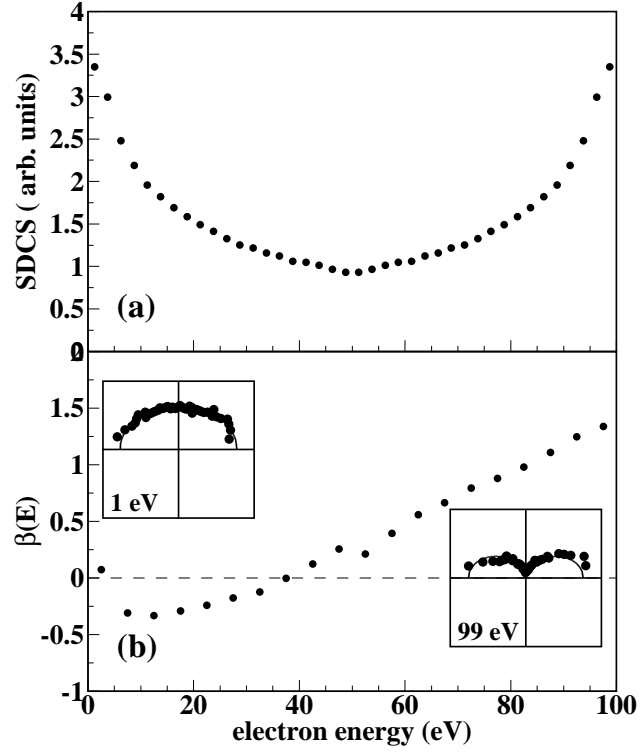


FIG. 2: (a) Electron energy distribution or single differential cross section ( $d\sigma/dE_1$ ). (b)  $\beta$ -parameter of one electron from helium double ionization at 179 eV photon energy. The insets show the DDCS  $d\sigma^2/(d\Omega dE)$  at  $E = 1$  eV and 99 eV in polar coordinates.

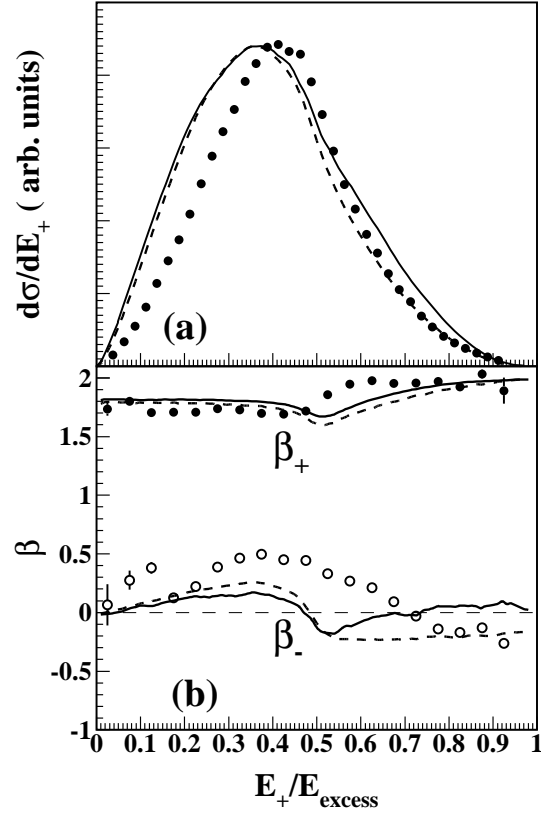


FIG. 3: (a)  $SDCS = d\sigma/dE_+$ , energy in units of the 100 eV excess energy. (b)  $\beta$ -parameter of the  $k_+$  and  $k_-$  momenta. The dots are the experimental data, the solid and dashed lines show 3C calculations in length and velocity form, respectively.